Biochemical and Biophysical Research Communications 410 (2011) 40–44

Contents lists available at ScienceDirect

Biochemical and Biophysical Research Communications

journal homepage: www.elsevier.com/locate/ybbrc

Hypoxia induces beta-amyloid in association with death of RGC-5 cells in culture

Juan Li [a,b,1], Zhizhang Dong [a,1], Bingqian Liu [a], Yehong Zhuo [a], Xuerong Sun [a], Zhikuan Yang [a], Jian Ge [a,*], Zhiqun Tan [b,c,*]

[a] State Key Laboratory of Ophthalmology, Zhongshan Ophthalmic Center, Sun Yat-sen University, Guangzhou 510060, China
[b] Department of Neurology, University of California Irvine School of Medicine, Irvine, CA 92697, USA
[c] Institute of Memory Impairments and Neurological Disorders, University of California Irvine School of Medicine, Irvine, CA 92697, USA

ARTICLE INFO

Article history:
Received 13 May 2011
Available online 24 May 2011

Keywords:
Beta-amyloid
Oxidative stress
RGC-5 cells
Hypoxia
Cell death

ABSTRACT

Beta-amyloid (Aβ) derived from amyloid precursor protein (APP) has been associated with retinal degeneration in Alzheimer's disease (AD) and glaucoma. This study examined whether hypoxia exposure induces Aβ accumulation in RGC-5 cells. While levels of APP mRNA and protein significantly increased in the cells, elevated abundance of Aβ was also observed in cells and culture medium between 12 or 24 and 48 h after 5% O_2 hypoxia treatment. Additionally, there is a close relationship between induction of APP and Aβ and intracellular accumulation of ROS along with loss of mitochondrial membrane potential followed by the death of RGC-5 cells in culture under hypoxia. These results suggest a possible involvement of APP and Aβ in the death of RGCs challenged by hypoxia.

1. Introduction

Aβ, a short peptide of 39–43 amino acid residues in length, is known as the major component of amyloid plaques in the brain of Alzheimer's disease (AD) [1]. The most common forms of Aβ are $Aβ_{1-40}$ and $Aβ_{1-42}$, which are derived from APP following the proteolytic cleavage mediated by the orchestration of a group of different enzymes [1,2]. Studies have shown that $Aβ_{1-40}$ is more abundant than $Aβ_{1-42}$ in AD brain, whereas $Aβ_{1-42}$ appears more fibrillogenic and toxic than $Aβ_{1-40}$ [3]. Aβ directly induces oxidative stress and causes both apoptotic and necrotic types of neuronal cell death *in vitro* and *in vivo* [4,5]. Since a decade ago, accumulation of Aβ has been associated with glaucomatous degeneration of retinal ganglion cell (RGC) [6]. Recently we and others have further demonstrated that Aβ deposition in the retina is associated with loss of RGC and thinning of entire retina in AD [7,8]. These findings suggest that Aβ might play an important role in the pathogenesis of retinal degeneration that is commonly found in glaucoma, AD, and other age-related vision impairments.

Retinal hypoxia is a common pathophysiological mechanism underlying a broad spectrum of sight-threatening disorders including glaucoma and ischemic occlusion of retinal artery or vein [9]. Systemic or neurological complications leading to retinal hypoperfusion such as diabetes and AD induce hypoxia in the retina as well [7,10]. In glaucoma, hypoxia is the major mediator responsible for RGC loss [9,11]. In addition to the direct toxicity to mitochondrial function, hypoxic or ischemic stress markedly induces accumulation of Aβ in the central nervous system both *in vivo* and *in vitro* through upregulating APP expression directly or altering other regulators in the metabolic pathways of APP and Aβ [12,13]. Until now it still remains unclear whether hypoxia directly induces Aβ accumulation in the retinal cells and its relevance for the death of RGCs. We therefore studied expression of APP along with accumulation of Aβ in RGC-5 cells in relation to cell death following hypoxia exposures.

2. Materials and methods

2.1. Cell culture and hypoxia treatment

The RGC-5 cell, a widely used cell line that has been characterized as expressing RGC markers and exhibiting ganglion cell-like behavior in culture [14], was a kind gift previously from Dr. Neeraj Agarwal (Department of Cell Biology and Genetics, UNT Health Science Center, Fort Worth, TX). Cells were grown in Dulbecco's modified Eagle's medium (DMEM) containing 10% fetal bovine

Abbreviations: APP, amyloid precursor protein; Aβ, beta-amyloid; AD, Alzheimer's disease; RGC, retinal ganglion cell; ROS, reactive oxygen species; ICC, immunocytochemistry; qRT-PCR, quantitative reverse transcription-polymerase chain reaction; ELISA, enzyme-linked immunosorbent assay; TUNEL, TdT-mediated dUTP nick end-labeling; PS, phospholipid phosphatidylserine; PI, propidium iodide; FITC, fluorescein isothiocyanate.

* Corresponding authors. Addresses: UCI School of Medicine/Neurology, 100 Irvine Hall, Zot 4275, Irvine, CA 92697-4275, USA. Fax: +1 949 824 3135 (Z. Tan), Zhongshan Ophthalmic Center, Sun Yat-sen University, 54 S. Xianlie Road, Guangzhou 510060, China (J. Ge).

E-mail addresses: gejian@mail.sysu.edu.cn (J. Ge), tanz@uci.edu (Z. Tan).

[1] The first two authors contributed equally to this work.

0006-291X/$ - see front matter © 2011 Elsevier Inc. All rights reserved.
doi:10.1016/j.bbrc.2011.05.101

serum, 2 mM GlutaMax (Invitrogen, Carlsbad, CA), 0.1% PenStrep (Invitrogen) in a humidified atmosphere containing 5% CO_2 at 37 °C. Cultured cells in 10 cm plates were split by trypsinization every 3 or 4 days. Cell passages within 10–20 were used for the experiments. The hypoxia condition was achieved by a hypoxia cell culture chamber (Stemcell Technologies, Vancouver, BC, Canada) with 5% O_2, 5% CO_2 and 90% N_2 supply regulated by an atmospheric pressure control system (Guangkong Automation Equipment Co., Guangzhou, China). For live cell assay and immunocytochemistry (ICC), cells were grown on 4-well chamber slides. Following 12–48 h cultured in the hypoxic condition, cells were either directly assayed or fixed with 4% paraformaldehyde for immunocytochemistry (ICC) or harvested for isolation of total RNA for qRT-PCR and preparation of whole cell lysates for Western blot. Cells cultured in normal air with 5% CO_2 were used as controls.

2.2. Immunocytochemistry

ICC on fixed cells was performed as described [15]. Briefly, cells were incubated with a universal blocking buffer to minimize non-specific binding prior to overnight incubation with a primary antibody diluted in 1 × PBS at 4 °C. Dilutions of primary antibodies were: Ab1, rabbit anti-APP (Affinity Bioreagents, Golden, CO), 1:100; 6E10, mouse anti-APP and Aβ (Covance, Denver, PA), 1:1000; and 12F4, mouse anti-$A\beta_{42}$ (Covance, Denver, PA), 1:2000. Immunoreactivity was examined by fluorescence microscopy following incubation with an Alexa Fluor 488- or 594-conjugated anti-mouse or rabbit secondary antibody (Invitrogen, 1:1000) and nuclear counterstaining using Hoechst 33342 (Invitrogen). A negative control was performed with omitting a primary antibody. Fluorescence micrographs were captured using a Zeiss LSM 510 confocal microscope or a Leica DLMB fluorescence microscope.

2.3. ELISA assay for $A\beta_{42}$

The levels of $A\beta_{42}$ in the cell culture medium were examined by ELISA using a commercial Rat $A\beta_{42}$ ELISA kit (Wako, Osaka, Japan) according to the manufacturer's protocol. This ELISA system uses monoclonal antibody BNT77, which recognizes an epitope of Aβ(11–28) and is precoated on 96-well surface for capture of $A\beta_{x-42}$, and monoclonal antibody BC05, which specifically detects the C-terminal portion of $A\beta_{42}$. 100 μl of cell culture medium from each sample was assayed in the study.

2.4. Western blot

Western blotting was conducted as described [15]. Briefly, about 35–40 μg total protein of cell lysates were denatured and resolved on a 10% SDS-poly acrylamide gel, transferred to a PVDF membrane (Millipore, Temecula, CA), briefly incubated in Blotto blocking buffer containing Tween 20 (0.1% v/v, PBST) and 5% (w/v) milk to block non-specific binding followed by overnight incubation with a primary antibody in 5% milk powder in PBST at 4 °C. Dilutions of primary antibodies were: mouse anti-GAPDH (mouse monoclonal IgG, Kangcheng, Shanghai, China), 1:500; and rabbit anti-APP polyclonal IgG (Cell Signaling, Danvers, MA), 1:500. The blotting results on the membranes were visualized by the enhanced chemiluminescence detection system (Cell Signaling, Danvers, MA) following 1 h incubation with a horse radish peroxidase-conjugated secondary antibody in RT and washing. Immunoblot pixel intensity was quantified using Image J software.

2.5. Real-time qRT-PCR

Total RNA was isolated using Trizol (Invitrogen) according to the manufacturer's instruction and treated with DNase I (Sigma, St. Louis, MO) to remove possible DNA contamination. cDNA was synthesized using the PrimeScript RT reagent Kit (Takara, Tokyo, Japan) following the manufacturer's manual. qRT-PCR was performed on an ABI Prism 7000 Real-Time PCR System (Applied Biosystems, Foster City, CA) using the SYBR Premix Ex Taq (Takara). A PCR reaction (20 μl) contained cDNA template (approximately 50 ng), SYBR Premix Ex Taq (10 μl), forward and reverse primers (0.2 μm each) for the control (β-actin, forward: 5′-GGAGAT TACTGCCCTGGCTCCTA-3′, reverse: 5′-GACTCATCGTACTCCTGCTTGCT G-3′) or APP (forward, 5′-CCAGCCAGTGACCATCCAGA-3′, reverse: 5′-GCATCGCTTACAAACT CACCA-3′), and ROX Reference Dye (0.4 μl). The PCR reactions were subjected to 40 cycles (95 °C, 10 s, 1×; 95 °C, 5 s, 60 °C, 31 s, 40×) followed by melting curve analysis and agarose gel resolution of PCR product to confirm the specificity of PCR reaction as described [15,16]. Following determination of the cycle threshold (CT) by the PCR system, the abundance of the interest gene related to the internal control of housekeeper (β-actin), was quantified using the ΔΔCT method as described [17], in which ΔCT is calculated from $CT_{interest} - CT_{\beta\text{-actin}}$ and $\Delta\Delta CT = \Delta CT_{interest} - \Delta CT_{control}$.

2.6. TdT-mediated dUTP nick end-labeling (TUNEL)

TUNEL was performed using an in situ cell death detection kit from Roche as described [15]. For double-labeling cells were incubated in blocking buffer for 30 min at room temperature followed by 6E10 antibody (1:1000) for Aβ and an Alexa Fluor 594-conjugated secondary antibody against mouse IgG (1:1000, Invitrogen) for microscopic visualization.

2.7. Measurement of intracellular ROS

Intracellular ROS was measured using a fluorescent probe orodihydrofluorescein diacetate (H2DCFDA, Invitrogen) as described [18]. Briefly, RGC-5 cells were grown in 35-mm-diameter Petri dishes at an initial density of 10^4 cells/ml and kept in the hypoxia chamber for indicated periods. The cells were washed with PBS twice prior to incubation with freshly prepared H2DCFDA (10 μM in medium) at 37 °C in dark for 30 min. Cells were then immediately analyzed following PBS wash twice by confocal microscopy (100 M; Carl Zeiss, Jena, Germany) at an excitation wavelength of 488 nm and an emission wavelength of 530 nm. The image results were quantified using Image-Pro-Plus software.

2.8. Flow cytometric analyses for mitochondrial membrane potential and annexin V binding

Mitochondrial membrane potential of cells was assayed using the fluorescent dye JC-1 (invitrogen) and quantified by flow cytometry. Briefly, treated cells were trypsinized and suspended at the density of 2×10^6 cells/ml and incubated with JC-1 (1 μg/ml) in serum-free DMEM for 30 min at 37 °C in dark. Cells were then rinsed twice with PBS and analyzed immediately in FACS-400 (BD Bioscience, San Jose, CA) at ex 488 nm, em 530 nm for green and em 590 nm for red fluorescence. Apoptosis in the RGC-5 following hypoxia was measured by using the Annexin V-FITC/PI Detection Kit (Keygen, Nanjing, China) according to the manufacturer's directions. RGC-5 cells were harvested, washed with PBS, re-suspended in the binding buffer from the kit (10^6 cells/ml), and mixed with annexin V-FITC (5 μl) and PI (5 μl). 15 min after incubation at RT in dark, cells were immediately analyzed by flow cytometry using FACS-400. The percentages of apoptotic or necrotic cells were determined from the number of annexin-V(+):PI(+) or annexin-V(−):PI(+) cells relative to the total number of cells, respectively.

All assays were performed in triplicate or up to five replica and data were expressed as the mean ± S.E.M. Statistical analysis was

performed using Student's *t*-test, one way ANOVA. A value of $p \leqslant 0.05$ was considered to be statistically significant.

3. Results

3.1. Hypoxia induces APP and Aβ proteins in RGC-5 cells in culture

Real-time qRT-PCR revealed a significant increase in APP mRNA level in RGC-5 cells starting at 24 h and almost quadrupled relative to β-actin control at 48 h after 5% oxygen hypoxia (Fig. 1A). This was further corroborated by the Western blots showing increased immunoreactivity of APP protein in the whole lysates of RGC-5 cells by 12 h after hypoxia (Fig. 1B), which followed same trend as APP mRNA induction and coincided with elevation of $A\beta_{42}$ levels in the culture media at corresponding time courses following hypoxia exposures. Immunocytochemistry using two specific antibodies against APP or Aβ revealed markedly increased immunoreactivity of APP as well as Aβ deposits 48 h after hypoxia (Fig. 1C). By contrast, only a very light basal level of APP, without Aβ, was detected in the control cells (Fig. 1D).

3.2. Hypoxia induces accumulation of ROS and mitochondrial stress in relation to death of RGC-5 cells in culture

Aβ triggers ROS production and mitochondrial stress, and ultimately leads to neuronal damage both structurally and functionally [19,20]. Normally ROS was undetectable in the control cells, whereas noticeably increased abundance of ROS was found 24–48 h in RGC-5 cells following hypoxia (Fig. 2A top row and B). Furthermore, when assayed with JC-1 fluorescent dye, a commonly used mitochondrial membrane potential indicator, flow cytometry revealed a dramatic loss of mitochondrial membrane potential in the cells along with time of hypoxia (Fig. 2A bottom row and C), suggesting mitochondrial stress and cell damage resulting from hypoxia. This was further corroborated by the detection of increased cell death with or without elevation of membrane phospholipid phosphatidylserine (PS) externalization as demonstrated by flow cytometric analysis following double-labeling with propidium iodide (PI) and FITC-annexin V (Fig. 3A). Importantly, double-label immunofluorescence microscopy further confirmed association of Aβ accumulation with cell death by the identification of $A\beta_{42}$ immunoreactivity in TUNEL-positive cells using dual immunofluorescence microscopy (Fig. 3C).

4. Discussion

Current study has demonstrated an increase in abundance of APP and Aβ peptides in RGC-5 cells following 5% oxygen hypoxia treatment. Increased protein level apparently results, at least in part, from transcriptional induction of APP gene [21,22], which is consistent with the observations in RGC-5 cells following chemical hypoxia mediated by cobalt chloride treatment [23]. There was a close correlation between accumulation of APP and Aβ and induction of ROS and mitochondrial stress, which was further linked with the sign of cell death demonstrated by the detection of annexin V externaliztion and the presence of TUNEL-stained nuclei consistent with apoptosis. Interestingly, the number of dying cells with absence of annexin V externalization was sharply increased at 48 h after hypoxia, at which Aβ abundance elevated both intra- and extra-cellularly. Previous studies have documented both necrotic and apoptotic types of cell death induced by Aβ, which were mainly through induction of ROS and mitochondrial stress, in the central nervous system [24]. In the present study accumulation of APP/Aβ and ROS along with a dramatic loss of mitochondrial membrane potential was simultaneously detected after certain hypoxia exposures. Our findings suggest a possible role of Aβ in the loss of RGCs in response to hypoxic stress. In fact, immunotherapy that targets Aβ efficiently ameliorated RGC loss in rats induced by elevated intraocular pressure [25] and protected retina from degeneration in AD mice (Li and Tan, unpublished observations). Additional studies are therefore warranted to characterize the temporal changes of APP and Aβ in matured RGCs and the

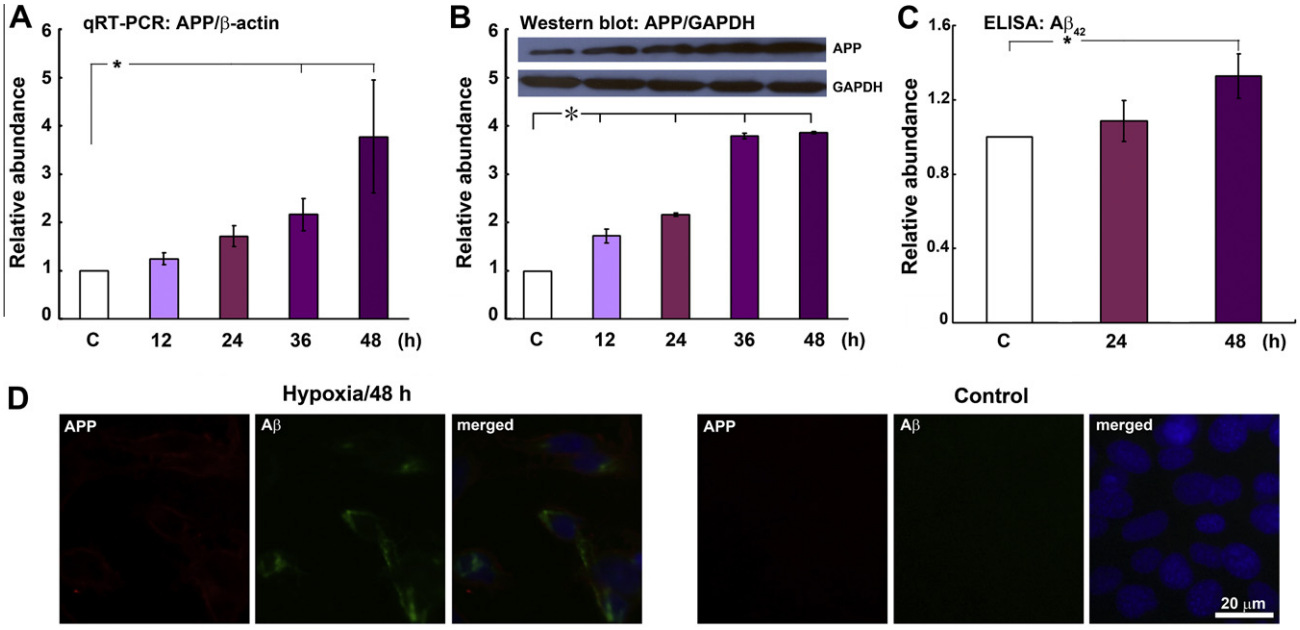

Fig. 1. Increased APP expression and Aβ in RGC-5 cells in culture under hypoxia. Induction of APP mRNA determined by real-time qRT-PCR (A) and APP protein by Western blotting (B) in RGC-5 cell in culture between 12 and 48 h under hypoxia. (C) ELISA reveals increase levels of Aβ in the culture media between 24 and 48 h under hypoxia. (D) Dual immunofluorescence detects increased immunoreactivity of APP (green) and Aβ (red) and a low background signal in RGC-5 cells 48 h after hypoxia and control, respectively. Nuclei were counterstained in blue with Hoechst 33342. Quantitation is depicted as mean ± S.E.M. at indicated times after hypoxia. C, control, $^{*}p < 0.05$, $N = 3$.

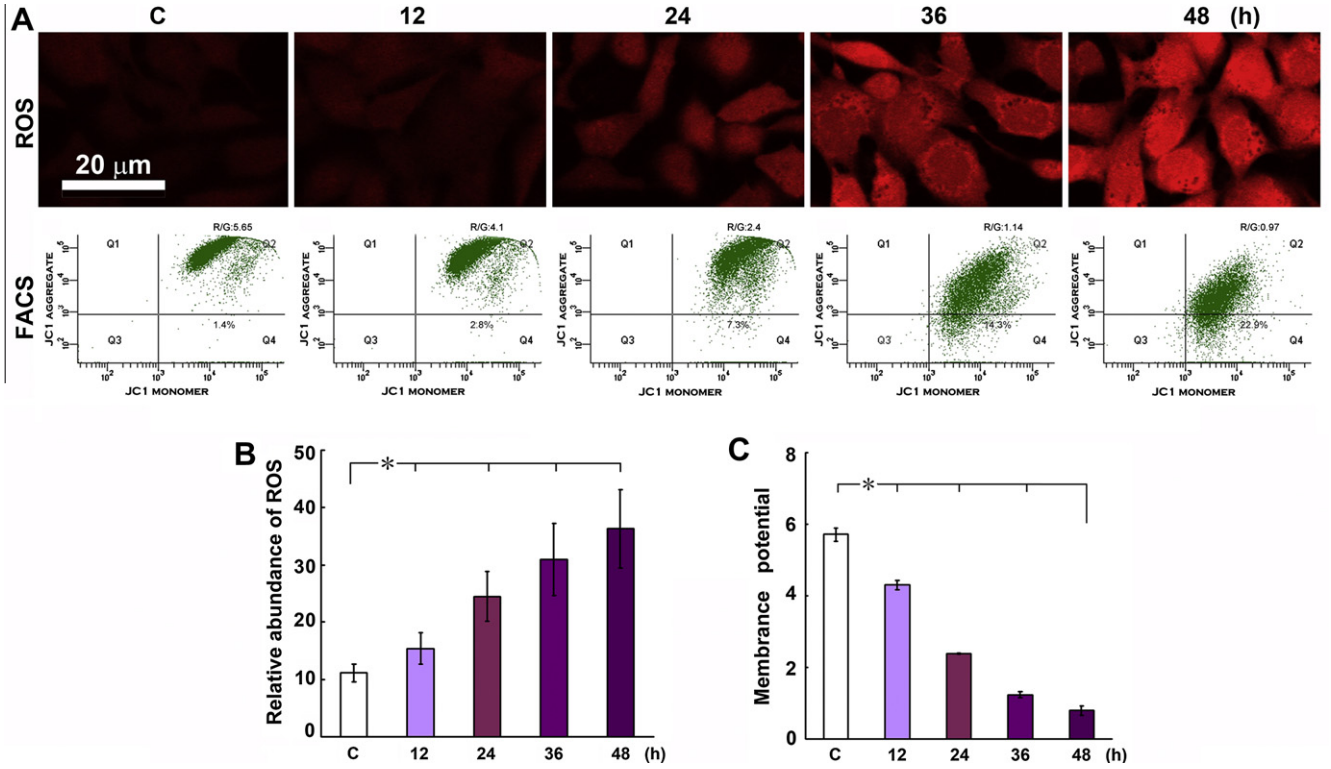

Fig. 2. Induction of ROS and changes in mitochondrial membrane potential in RGC-5 cells by hypoxia. (A) Intracellular accumulation of ROS detected by fluorescence microscopy following H2DCFDA labeling (top row) and loss of mitochondrial membrane analyzed by FACS following JC-1 staining (bottom row) in RGC-5 cells under hypoxia. Relative abundance of ROS (B) and the results of FACS analysis (C) are quantified and depicted as mean ± S.E.M.. $^{*}p < 0.05$.

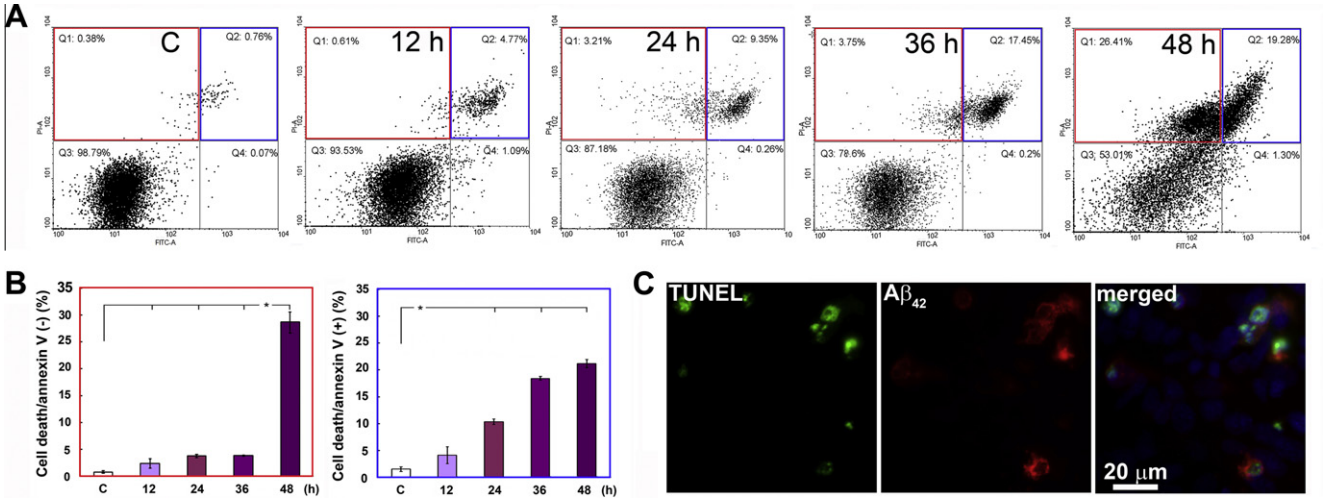

Fig. 3. Death of RGC-5 cells is associated with Aβ in culture under hypoxia. (A). Flow cytometry demonstrates increased both annexin-V-negative (Q1, red box) and annexin-V-positive (Q2, blue box) in cells following annexin-V-FITC/PI labeling at indicated times after hypoxia. (B) Quantitation of annexin-V-negative (left panel) and annexin-V-positive (right panel) cell death indicates remarkable increases in two different types of cell death under hypoxia. The results are depicted as mean ± S.E.M.. C, control. $^{*}p < 0.05$, $N = 4–5$. (C) Double-label immunofluorescence reveals TUNEL-positive (green) cells with prominent Aβ immunoreactivity (red).

relevance for RGC loss *in vivo* under glaucomatous or other ischemic conditions.

In conclusion, the present study has clearly demonstrated induction of APP and Aβ associated with accumulation of ROS and mitochondrial stress along with death of RGC-5 cells in culture under hypoxia. These observations provide further support for a possible role of APP and Aβ in the pathogenesis of glaucoma as well as other neurodegenerative disorders in the retina.

Acknowledgments

The study was supported by the National Basic Research Program of China (2007CB512200) and the Natural Science Foundation of China (30973266), and the Guangdong Natural Science Foundation (9451008901001999) to J.G., and Alzheimer's Drug Discovery Foundation (290202) to Z.T.. J.L. was supported by China Scholarship Council's Scholarship program (2009638043).

References

[1] J. Hardy, D.J. Selkoe, The amyloid hypothesis of Alzheimer's disease: progress and problems on the road to therapeutics, Science 297 (2002) 353–356.

[2] D.J. Selkoe, Amyloid beta-protein and the genetics of Alzheimer's disease, J. Biol. Chem. 271 (1996) 18295–18298.

[3] S.S. Sisodia, D.L. Price, Role of the beta-amyloid protein in Alzheimer's disease, FASEB J. 9 (1995) 366–370.

[4] D.T. Walsh, R.M. Montero, L.G. Bresciani, A.Y. Jen, P.D. Leclercq, D. Saunders, E.L.-A. AN, L. Gbadamoshi, S.M. Gentleman, L.S. Jen, Amyloid-beta peptide is toxic to neurons *in vivo* via indirect mechanisms, Neurobiol. Dis. 10 (2002) 20–27.

[5] J. Carter, C.F. Lippa, Neuronal death and Alzheimer's disease, Beta-amyloid, Curr. Mol. Med. 1 (2001) 733–737.

[6] S.J. McKinnon, D.M. Lehman, L.A. Kerrigan-Baumrind, C.A. Merges, M.E. Pease, D.F. Kerrigan, N.L. Ransom, N.G. Tahzib, H.A. Reitsamer, H. Levkovitch-Verbin, H.A. Quigley, D.J. Zack, Caspase activation and amyloid precursor protein cleavage in rat ocular hypertension, Invest. Ophthalmol. Vis. Sci. 43 (2002) 1077–1087.

[7] B. Liu, S. Rasool, Z. Yang, C.G. Glabe, S.S. Schreiber, J. Ge, Z. Tan, Amyloid-peptide vaccinations reduce {beta}-amyloid plaques but exacerbate vascular deposition and inflammation in the retina of Alzheimer's transgenic mice, Am. J. Pathol. 175 (2009) 2099–2110.

[8] A. Ning, J. Cui, E. To, K.H. Ashe, J. Matsubara, Amyloid-beta deposits lead to retinal degeneration in a mouse model of Alzheimer disease, Invest. Ophthalmol. Vis. Sci. 49 (2008) 5136–5143.

[9] C. Kaur, W.S. Foulds, E.A. Ling, Hypoxia-ischemia and retinal ganglion cell damage, Clin. Ophthalmol. 2 (2008) 879–889.

[10] T.M. Curtis, T.A. Gardiner, A.W. Stitt, Microvascular lesions of diabetic retinopathy: clues towards understanding pathogenesis?, Eye (Lond) 23 (2009) 1496–1508

[11] K.G. Schmidt, L.E. Pillunat, N.N. Osborne, [Ischemia hypoxia. An attempt to explain the different rates of retinal ganglion cell death in glaucoma], Ophthalmologe 101 (2004) 1071–1075.

[12] L. Li, X. Zhang, D. Yang, G. Luo, S. Chen, W. Le, Hypoxia increases a beta generation by altering beta- and gamma-cleavage of APP, Neurobiol. Aging 30 (2009) 1091–1098.

[13] X. Sun, G. He, H. Qing, W. Zhou, F. Dobie, F. Cai, M. Staufenbiel, L.E. Huang, W. Song, Hypoxia facilitates Alzheimer's disease pathogenesis by up-regulating BACE1 gene expression, Proc. Natl. Acad. Sci. USA 103 (2006) 18727–18732.

[14] R.R. Krishnamoorthy, P. Agarwal, G. Prasanna, K. Vopat, W. Lambert, H.J. Sheedlo, I.H. Pang, D. Shade, R.J. Wordinger, T. Yorio, A.F. Clark, N. Agarwal, Characterization of a transformed rat retinal ganglion cell line, Brain Res. Mol. Brain Res. 86 (2001) 1–12.

[15] Z. Tan, W. Qu, W. Tu, W. Liu, M. Baudry, S.S. Schreiber, p53 accumulation due to down-regulation of ubiquit: relevance for neuronal apoptosis, Cell Death Differ. 7 (2000) 675–681.

[16] X. Zhang, W. Le, Pathological role of hypoxia in Alzheimer's disease, Exp. Neurol. 223 (2010) 299–303.

[17] M.W. Pfaffl, A new mathematical model for relative quantification in real-time RT-PCR, Nucleic Acids Res. 29 (2001) e45.

[18] Y. He, K.W. Leung, Y.H. Zhang, S. Duan, X.F. Zhong, R.Z. Jiang, Z. Peng, J. Tombran-Tink, J. Ge, Mitochondrial complex I defect induces ROS release and degeneration in trabecular meshwork cells of POAG patients: protection by antioxidants, Invest. Ophthalmol. Vis. Sci. 49 (2008) 1447–1458.

[19] P. Sompol, W. Ittarat, J. Tangpong, Y. Chen, I. Doubinskaia, I. Batinic-Haberle, H.M. Abdul, D.A. Butterfield, D.K. St Clair, A neuronal model of Alzheimer's disease: an insight into the mechanisms of oxidative stress-mediated mitochondrial injury, Neuroscience 153 (2008) 120–130.

[20] M.P. Mattson, D.S. Gary, S.L. Chan, W. Duan, Perturbed endoplasmic reticulum function, synaptic apoptosis and the pathogenesis of Alzheimer's disease, Biochem. Soc. Symp. (2001) 151–162.

[21] R. Vassar, The beta-secretase, BACE: a prime drug target for Alzheimer's disease, J. Mol. Neurosci. 17 (2001) 157–170.

[22] J.J. Palacino, B.E. Berechid, P. Alexander, C. Eckman, S. Younkin, J.S. Nye, B. Wolozin, Regulation of amyloid precursor protein processing by presenilin 1 (PS1) and PS2 in PS1 knockout cells, J. Biol. Chem. 275 (2000) 215–222.

[23] X. Zhu, W. Zhou, Y. Cui, L. Zhu, J. Li, Z. Xia, B. Shao, H. Wang, H. Chen, Muscarinic activation attenuates abnormal processing of beta-amyloid precursor protein induced by cobalt chloride-mimetic hypoxia in retinal ganglion cells, Biochem. Biophys. Res. Commun. 384 (2009) 110–113.

[24] K. Andersson, A. Olofsson, E.H. Nielsen, S.E. Svehag, E. Lundgren, Only amyloidogenic intermediates of transthyretin induce apoptosis, Biochem. Biophys. Res. Commun. 294 (2002) 309–314.

[25] L. Guo, T.E. Salt, V. Luong, N. Wood, W. Cheung, A. Maass, G. Ferrari, F. Russo-Marie, A.M. Sillito, M.E. Cheetham, S.E. Moss, F.W. Fitzke, M.F. Cordeiro, Targeting amyloid-beta in glaucoma treatment, Proc. Natl. Acad. Sci. USA 104 (2007) 13444–13449.